Molecular Therapy
Nucleic Acids
Original Article

Shorter Phosphorodiamidate Morpholino Splice-Switching Oligonucleotides May Increase Exon-Skipping Efficacy in DMD

Ugur Akpulat,[1,2,3] Haicui Wang,[1,2] Kerstin Becker,[1,2] Adriana Contreras,[1,2] Terence A. Partridge,[4,5] James S. Novak,[4,5] and Sebahattin Cirak[1,6]

[1]Center for Molecular Medicine Cologne (CMMC), University of Cologne, Cologne 50931, Germany; [2]Department of Pediatrics, University Hospital Cologne, Cologne 50937, Germany; [3]Department of Medical Biology, Faculty of Medicine, Kastamonu University, Kastamonu 37100, Turkey; [4]Center for Genetic Medicine Research, Children's Research Institute, Children's National Health System, Washington, DC 20010, USA; [5]Department of Genomics and Precision Medicine, The George Washington University School of Medicine and Health Sciences, Washington, DC 20010, USA

Duchenne muscular dystrophy is a fatal muscle disease, caused by mutations in *DMD*, leading to loss of dystrophin expression. Phosphorodiamidate morpholino splice-switching oligonucleotides (PMO-SSOs) have been used to elicit the restoration of a partially functional truncated dystrophin by excluding disruptive exons from the *DMD* messenger. The 30-mer PMO eteplirsen (EXONDYS51) developed for exon 51 skipping is the first dystrophin-restoring, conditionally FDA-approved drug in history. Clinical trials had shown a dose-dependent variable and patchy dystrophin restoration. The main obstacle for efficient dystrophin restoration is the inadequate uptake of PMOs into skeletal muscle fibers at low doses. The excessive cost of longer PMOs has limited the utilization of higher dosing. We designed shorter 25-mer PMOs directed to the same eteplirsen-targeted region of exon 51 and compared their efficacies *in vitro* and *in vivo* in the *mdx*52 murine model. Our results showed that skipped-dystrophin induction was comparable between the 30-mer PMO sequence of eteplirsen and one of the shorter PMOs, while the other 25-mer PMOs showed lower exon-skipping efficacies. Shorter PMOs would make higher doses economically feasible, and high dosing would result in better drug uptake into muscle, induce higher levels of dystrophin restoration in DMD muscle, and, ultimately, increase the clinical efficacy.

INTRODUCTION

Duchenne muscular dystrophy (DMD) is a severe, X-linked, recessive muscle disease caused by frameshifting or nonsense mutations in the dystrophin gene (*DMD*) that lead to progressive muscle weakness and death by respiratory and cardiac failure in the second or third decade of life. There is an unmet medical need for the treatment of this lethal disorder. *DMD* is the largest known human gene, with 79 exons spanning about 2.3 Mb of genomic DNA on the X chromosome and encoding a 14-kb mRNA.[1,2] Intragenic deletions are the most common mutations in *DMD*, encompassing one or more exons and accounting for approximately two-thirds of patients. *DMD* with open-reading-frame-disrupting mutations results in marked dystrophin deficiency in all muscles of patients with DMD.[3] Dystrophin is a structural protein that localizes beneath the sarcolemma and connects the cytoskeleton of muscle fibers to the surrounding basal lamina as a part of the dystrophin-associated glycoprotein complex (DGC).[4,5] The absence of dystrophin destabilizes the DGC and results in a large reduction of DGC components, rendering the sarcolemma susceptible to damage from muscle contraction and leading to a loss of critical signaling events governed by the DGC.[6] The allelic disorder, Becker muscular dystrophy (BMD), has a milder disease progression since the causative mutations maintain the *DMD* open reading frame and result in an internally truncated but partially functional protein. BMD patients show variable phenotypes, ranging from asymptomatic to severe, which depend on the mutation and the resulting protein defect.[7]

Chemically modified splice-switching oligonucleotides (SSOs) are used to interfere with the splicing process of a specific pre-mRNA by binding to *cis*-acting splicing regulatory elements to exclude reading-frame-disrupting exons from the mature transcript. The restoration of the reading frame by SSOs results in the expression of a shorter dystrophin protein, which lacks some internal spectrin domains but retains the crucial functional elements, resembling the situation in BMD patients. Extensive clinical experience has been gained by the systemic administration of SSOs in patients with DMD who have mutations amenable to exon 51 skipping. This constitutes about 13% of all the DMD patients and the largest DMD group. Dystrophin-restoring therapies are currently in clinical development, including exon-skipping approaches with SSOs.[8,9] Exon skipping is a mutation-specific personalized medicine approach and

Received 20 April 2018; accepted 4 October 2018;
https://doi.org/10.1016/j.omtn.2018.10.002.

[6]Present address: Department of Pediatrics, University Hospital Cologne, Cologne 50937, Germany.

Correspondence: Sebahattin Cirak, MD, Department of Pediatrics, University Hospital Cologne, Cologne 50937, Germany.
E-mail: sebahattin.cirak@uk-koeln.de

covers potentially 70% of all patients with DMD.[10,11] The proof of principle was demonstrated in the *mdx* mouse model of DMD and DMD-patient-derived myoblasts.[12,13] Both studies had shown dystrophin expression with the proper localization, and preclinical *in vitro* studies had confirmed an internal region within exon 51 of *DMD* as the most effective target candidate for exon 51 skipping.[14,15] This region has been targeted in preclinical animal model studies and clinical trials mainly with two different SSO backbones, the 2′ O-methyl phosphorothioate (2OMePS) backbone and the phosphorodiamidate morpholino (PMO) backbone.[8,16] These backbone chemistries drive their pharmacokinetic properties, safety, and tolerability.[17] In early 2016, the U.S. Food and Drug Administration (FDA) rejected the approval of drisapersen due to an insufficient clinical benefit and toxicity issues that limited dosing[18] (https://www.drugs.com/history/kyndrisa.html). In contrast, eteplirsen has shown to be safe, but rapid clearance from circulation seems to limit its efficient delivery to muscle fibers.[19] However, there is a controversial debate in the scientific literature on exon-skipping efficacy.[19,20] The FDA conditionally approved EXONDYS51 (eteplirsen), developed for exon 51 skipping of *DMD* pre-mRNA, on the basis of the surrogate endpoint of dystrophin restoration in skeletal muscles of patients with DMD. However, the limited evidence of functional clinical benefits caused a debate due to the low sample size of 12 patients and the open-label study[8,9] (FDA application no. 206488Orig1s000).

Systemic delivery of eteplirsen to patients with DMD has been shown to induce dose-dependent, low-level dystrophin restoration; however, a variable and patchy dystrophin expression was also observed.[8,9] Importantly, restoration of dystrophin by eteplirsen showed relocalization of DGC proteins, including neuronal NOS, to the sarcolemma of myofibers.[8,21]

The low-level expression of dystrophin observed in clinical trials with eteplirsen may have likely limited the clinical benefit. Asymptomatic patients with BMD have relatively more dystrophin expression than patients with mild or severe BMD.[7] Moreover, in *mdx* mice, higher doses of PMOs correlated with greater expression of dystrophin, with a concomitant reduction in degenerated regions, reduced inflammatory infiltrates in the diaphragm, and almost abolished the muscular dystrophy.[22,23] In order to increase the amount of restored dystrophin, an obvious approach would be to increase the PMO dose that is administered. Preclinical studies with cynomolgus monkeys revealed that increasing the dose of eteplirsen up to 10-fold that had been used in clinical trials was well tolerated, with no observable serious adverse effects in the short term.[24]

The relatively short half-life of PMOs in plasma (1.62–3.60 hr), together with the recent finding that its uptake is restricted to actively regenerating myofibers, seems to limit its overall efficacy at lower doses, which had been used in the clinical trials so far.[8,25] In clinical trials, the level of restored dystrophin by western blot was 0.93% in eteplirsen-treated DMD patients after 180 weeks of administration, compared to healthy individuals (FDA application no. 206488Orig1s000). Since the amount of dystrophin required for substantial clinical benefit in DMD patients was estimated to be least 10% of normal levels with body-wide distribution, the restored dystrophin levels observed in clinical trials currently by eteplirsen are rather suboptimal.[26]

On the other hand, the excessive cost of eteplirsen, about $300,000 per patient annually, limits the administration of high doses to DMD patients (https://www.raredr.com/news/duchenne-drug-to-cost-300k). To overcome the dose limitation, we investigated whether the use of shorter PMOs may also be efficient in exon skipping in DMD, since shorter PMO-SSOs make higher dosing economically feasible. We used shorter 25-mer PMOs targeting the same region on exon 51 as the PMO sequence of eteplirsen and compared their efficacies on a dystrophin-null, exon-52-deleted H2K-*mdx*52 mouse myoblast cell line and in the *mdx*52 dystrophin-null mouse model.

RESULTS

Dose-Response *In Vitro* Exon-Skipping Assay

In order to establish an experimental quantitative exon-skipping assay aiming to show that 25-mer PMOs were sufficient and equivalent to 30-mer PMOs, we first used PMOE23 for skipping of exon 23 in H2K-*mdx*23 myoblasts. Two *Dmd* mRNA amplicons were observed on agarose gels (Figure S1), with the 519-bp amplicon corresponding to a *Dmd* transcript including exon 23 (unskipped) and the shorter 306-bp amplicon lacking the exon 23 (skipped), which was further validated as the skipped transcript by Sanger sequencing (Figure S2). Nested RT-PCR analysis revealed that exon 23 was skipped by PMOE23 in a dose-dependent manner, with the highest efficacy at 3,000 nM and the lowest efficacy at 300 nM. Neither a skipped band nor unspecific bands were observed in cells treated with less than 300 nm PMOE23 or in cells that were treated with scramble PMO (Figure S1). Expression of alpha-actinin in both cells transfected with either scrambled PMO or PMOE23 confirmed that the transfection and also the different doses of PMO tested do not impair proper myogenic differentiation (Figure S1).

25-mer PMOs for Exon 51 Skipping

We designed three shorter PMOs, targeting the same exon 51 region on the *Dmd* as the PMO sequence of eteplirsen (Etep) but 5 bp shorter (25-mer). Etep-Upstream corresponds to the first 25 bases from the 5′ end of Etep, Etep-Middle covers from the 4th to the 28th base of the Etep sequence, and Etep-Downstream matches the last 25 bases of Etep (Figure 1B). H2K *mdx*52 myoblasts were transfected with Etep or the shorter PMOs to determine and compare the effective doses for exon 51 skipping. Expression of alpha-actinin validated that neither transfection conditions nor the different doses of each PMO tested impaired or affected proper myogenic differentiation (Figure 2). Nested RT-PCR of the *Dmd* transcript generated two different amplicons: a 422-bp amplicon that corresponds to the *Dmd* transcript containing exon 51 (unskipped) and a 189-bp amplicon that corresponds to the *Dmd* transcript lacking exon 51 (skipped) (Figures 1A and 2). The shorter band was validated by Sanger sequencing as the skipped amplicon (Figure S2). Both Etep and the shorter PMOs showed similar exon-51-skipping activity. All of them skipped exon 51 in a

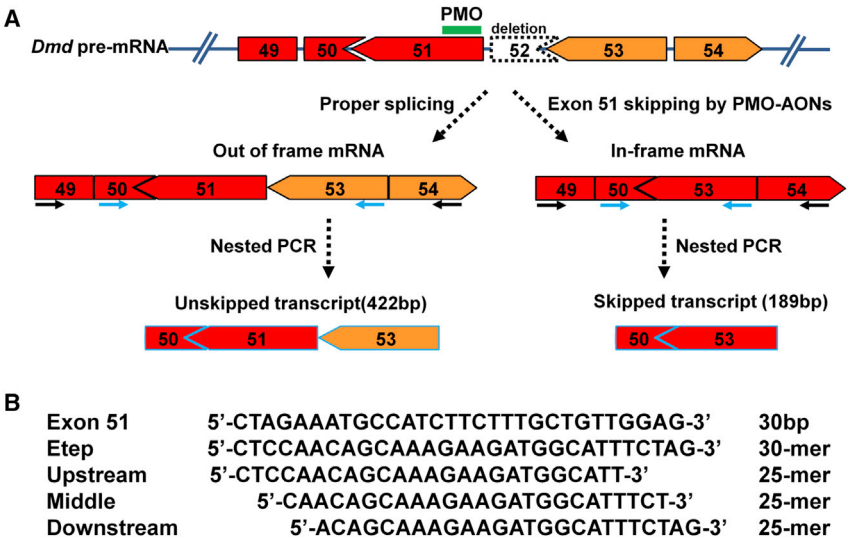

Figure 1. Representation of Exon 51 Skipping in *Dmd* Pre-mRNA by PMO-SSOs in H2K-*mdx*52 Cells

(A) Schematic depiction of *Dmd* pre-mRNA indicates the relative positions of exons (boxes with numbers), flanking introns (blue lines), disruption of the reading frame by the deletion of exon 52 in the H2K-*mdx*52 cell line, and relative position of the binding site to the PMOs on exon 51 (green line). The exon 52 deletion disrupts the open reading frame. Skipping of exon 51 by Etep and the shorter PMOs restores the downstream reading frame of *Dmd* mRNA. Arrows on *Dmd*-mRNAs indicate relative positions of the primers for the nested PCR (black arrows indicate outer primers, and blue arrows indicate inner primers). Nested PCR generates two amplicons, which correspond to unskipped mRNA (422 bp) and skipped mRNA (189 bp). (B) The target sequence within exon 51 of *Dmd* pre-mRNA and sequences of Etep and shorter PMOs with binding positions. The PMOs are antisense compounds that have reverse-complementary sequences to the target sequence within exon 51.

dose-dependent manner, with 100 nM as the lowest PMO concentration that exhibited skipping (Figures 2A and S3).

Quantification of the relative intensity of the bands corresponding to skipped and unskipped transcripts were performed to assess PMO-induced exon-51-skipping efficacy. The best skipping efficacy was observed for Etep, ranging from 9.5 to 78.5% skipping. The efficacy of Etep-Upstream was comparable with that of Etep, between 10.9 and 72.9%, while Etep-Middle and Etep-Downstream showed lower efficacies than those of Etep and Etep-Upstream and ranged between 4.3% and 41.9% and between 4.5% and 58%, respectively (Figure 3A).

In order to identify whether the dose of each PMO is able to induce equal amounts of skipped and unskipped *Dmd* mRNA, dose-response curves of normalized relative expressions of both *Dmd* transcripts were plotted on the same graph (Figure 3B). The intersection point of the two curves was determined as the PMO concentration that gives rise to equal expression. These calculations revealed that approximately 900 nM Etep yielded equal amounts of skipped and unskipped transcripts under experimental conditions, while, for the shorter PMOs, 1,260 nM Etep-Upstream, 2,530 nM Etep-Downstream, and 3,370 nM Etep-Middle were required. Altogether, these analyses showed that skipping of *Dmd* exon 51 by PMOs is inducible in a dose-dependent manner and that the shorter PMOs achieve a skipping effect comparable to that of the 30-mer PMOs at higher concentrations. We found that targeting the same sequence on the pre-mRNA with PMOs that have 5-nt differences results in different skipping efficacies. Higher concentrations up to 10 μM of the PMOs were also tested to examine whether the shorter PMOs might be able to saturate and reach the Etep exon-51-skipping activity levels if the concentration increases. While Etep-Upstream and Etep-Downstream reached the same efficacy as Etep at the 10-μM concentration, Etep-Middle showed considerably lower activity (Figure 2B).

Ultimately, we validated the restoration of dystrophin protein expression by shorter PMOs in the dystrophin-null *mdx*52 mice. The tibialis anterior (TA) muscles of *mdx* mice were injected intramuscularly with 5 μg and 20 μg of each PMO. Samples were collected for immunofluorescence analysis of dystrophin 2 weeks after injection. Both doses of all PMOs induced dystrophin expression. Widely distributed dystrophin-expressing myofibers confirmed the ability of shorter PMOs to induce dystrophin restoration *in vivo* (Figure 4). The percentage of dystrophin-positive fibers ranged from 3.8 to 14.0, but no significant difference was found between different PMOs and different doses of each PMO (Table S2). Additionally, dystrophin expression levels of dystrophin-positive fibers were compared among the treatment groups. The 5-μg and 20-μg doses of each PMO yielded similar dystrophin expression levels per dystrophin-positive fiber, indicating that, already at 5 μg, we reached a local intramuscular saturation (Figure S4). Local saturation provides an experimental system that allows us to test the effect of the PMO sequences on dystrophin restoration *in vivo*, since the PMO sequences are the only variable after local PMO saturation of muscle. Indeed, dystrophin restoration levels by the PMOs *in vivo* were comparable with the exon-skipping efficacies of the PMOs at high doses *in vitro* (Figures 5 and S4; Table S3). Etep-Upstream and Etep-Downstream showed dystrophin intensities in dystrophin-positive fibers that were similar to those of Etep, but Etep-Middle showed considerably lower dystrophin induction. The *in vivo* dystrophin intensity analyses of the dystrophin-positive fibers validated the effect of the sequence design on exon-skipping efficacy and are consistent, with our *in vitro* results.

DISCUSSION

In the present study, we used shorter PMOs as a new alternative to reduce the cost of PMO synthesis in order to permit higher doses at the same or lower economic costs as eteplirsen. Using higher doses of shorter PMOs may increase dystrophin restoration. We used three different 25-mer PMOs that target the same region of *Dmd* exon 51

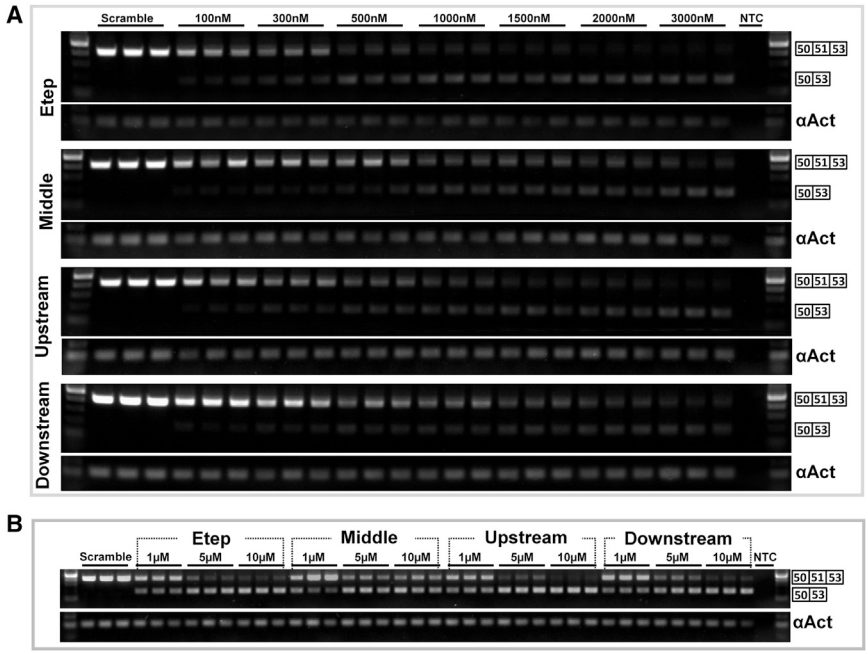

Figure 2. Nested RT-PCR Analysis of the Transfected H2K *mdx52* Cells Showing Exon 51 Skipping Induced by the Etep and the Shorter PMOs

Following 24 hr of induction of differentiation, the cells were transfected with the indicated concentrations of the PMOs, and skipping efficacy was analyzed 48 hr post-transfection. Agarose gel electrophoresis shows unskipped and exon-51-skipped transcripts of *Dmd* (illustrated by boxes with exon numbers). Biological triplicates were performed for each condition. Alpha-actinin (αAct) amplification indicates the proper differentiation of myoblasts to myotubes. First and last lines indicate the DNA ladder (a 100-bp ladder), and NTC is the non-template control. All PMOs exhibited a concentration-dependent increase in exon 51 skipping. (A) Transfection at concentrations ranging from 100 nM to 3,000 nM. (B) Transfection at concentrations ranging from 1 μM to 10 μM.

pre-mRNA as the PMO sequence of eteplirsen (Etep) with 2–3 bases shifting along the binding site of Etep (Figure 1B). Our results indicate that there is a dose-dependent interaction between the target sequence and PMOs; higher doses of the PMOs result in a greater skipping activity. In order to compare the PMO efficacies, we used two different evaluation methods: first, a comparison of the exon-skipping percentages after treatment; and, second, we measured the dose required for the different PMOs to reach the equivalent amounts of skipped and unskipped transcripts. Among the four PMOs, Etep and Etep-Upstream showed the highest and most comparable skipping percentages, while the other two had considerably lower values (Figure 3A). Using the second method by plotting the overlap between the dose-response curves for the skipped and unskipped transcripts, we determined the intersection point of the curves as the dose of 50% exon skipping; we name this PMO concentration the PMO_{50}. Similar PMO_{50} levels were obtained for Etep and Etep-Upstream, but the other two shorter PMOs required much higher doses to reach the PMO_{50} intersection (Figure 3B). Our calculation indicated that the dose-response relationship between PMOs and target sequences is not linear. One possible reason for the non-linear response could be that the competition between splice regulatory factors and PMO-SSOs to the target mRNA sequence may deviate from the proportional skipping response. Splicing occurs together with transcription, and co-transcriptional pre-mRNA folding leads to transient secondary structures. These transient pre-mRNA secondary structures are real targets for both the SSOs and the splicing factors. In order to exhibit their skipping ability, SSOs should bind to target sites before the splicing regulatory factors.[27,28] To test whether exon-skipping saturation could be also achieved by shorter PMOs, we also tested the exon-skipping efficacies of the PMOs at higher concentrations (Figure 2B). Etep-Downstream reached, at a 10-μM transfection concentration, the same exon-skipping efficacy as those of Etep-Upstream and Etep.

Our *in vitro* data indicate that shortening the length of PMOs to reduce the cost of treatment may yield the same efficacy as longer PMOs if higher doses are used. However, positioning the shorter PMOs along the target sequence has a great influence on exon-skipping efficacy. Even though the 25-mer PMOs only had 2- to 3-base differences in their sequence design, each of the shorter PMOs exhibited a different exon-skipping efficacy (Figure 3). Several reasons may explain this observation, such as the accessibility of the target sequence due to the physical pre-mRNA conformation, competition with splice regulatory factors, and the stability of the hetero-duplex between the target sequence and the SSO.[29] Determining the optimal SSOs for exon skipping has drawn specific attention due to the insufficient outcomes in clinical trials.[30–32] By using *in silico* prediction tools and *in vitro* screening approaches, Echigoya et al. have defined 30-mer PMOs with better exon-skipping efficacy than eteplirsen; these PMOs targets the initial 5′ site of the exon 51 instead of the internal region targeted by eteplirsen.[30] However, shortening the length of their best effective PMO from a 30-mer to a 25-mer resulted in less efficient skipping.[30] One reason for the reduced efficacy might be improper positioning along the candidate target sequence; another reason might be that distinct target sequences have their own skipping constraints.[33,34] In addition to the *in vitro* efficacy testing of shorter PMOs, we validated the dystrophin restoration by the shorter 25-mer-PMOs via intramuscular injections into the dystrophin-null *mdx52* mice (Figure 4). We used two approaches to compare the dystrophin restoration efficacy. While the percentage of the dystrophin-positive fibers did not show a significant difference between the PMOs (Table S2), the semiquantitative dystrophin intensity analyses of dystrophin-positive fibers revealed an effect of sequence design on dystrophin restoration (Figures 5 and S4; Table S3). The intramuscular injection approach for PMO testing has some technical challenges, including unequal distribution of the PMOs along the muscle and precise sectioning of the injected region, but

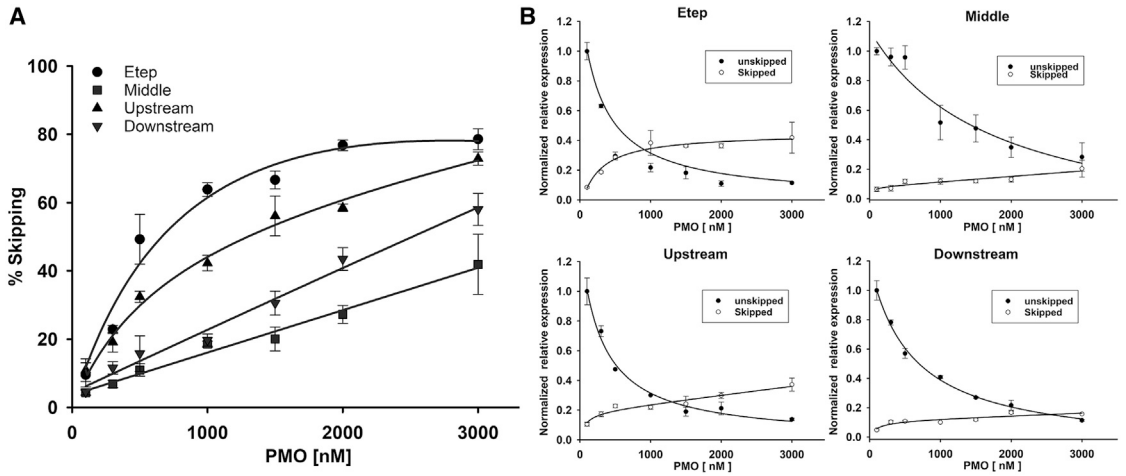

Figure 3. Exon-51-Skipping Efficacies of Etep and the Shorter PMOs in the H2K *mdx*52 Cells

Agarose gel band intensities of PCR products of *Dmd* and alpha-actinin were quantified from the corresponding gels (Figure 2A). (A) Percentage of exon 51 skipping induced by each PMO at different concentrations. Skipping percentages were calculated as (normalized relative expression of the skipped transcript/[normalized relative expression of the skipped + normalized relative expression of the unskipped transcripts]) × 100. (B) Dose-response curves of normalized relative expressions of skipped and unskipped *Dmd* transcripts for the PMOs. The curves of the *Dmd* transcripts were plotted on the same graphic for each PMO to show and compare the relative expression levels of skipped and unskipped transcripts in response to different concentrations of PMOs. Error bars represent SD.

it also has some advantages. Additionally, the intramuscular injection that differs from intravenous administration leads to local saturation of the PMOs at the injected region of the muscles. This may explain why the comparison of the percentage of dystrophin-positive fibers didn't show significant differences, and this usually not observed when the PMOs are administered intravenously, because of the dilution and elimination of the PMOs in the circulation due to the short half-life of PMOs. This local saturation may explain that different doses of the same PMOs (5 μg and 20 μg) resulted in the similar dystrophin intensity values of dystrophin-positive fibers. The advantage of this local PMO saturation is that PMO sequences are the main variable parameter for exon skipping and dystrophin restoration in the intramuscular system, thus suitable for the aim to compare different PMO-SSOs sequences in their skipping efficacy. Semiquantitative fluorescence intensity analysis of dystrophin signal intensity confirmed our *in vitro* experiments by indicating that 25-mer Etep-Upstream can induce similar dystrophin levels as 30-mer-PMO Etep (Figures 4, 5, and S4; Table S3). We demonstrate the importance of the sequence design of the PMOs for efficient dystrophin restoration. This positive *in vivo* examination further supports the feasibility of shorter PMOs for exon-skipping treatments. Shorter PMOs provide an opportunity to use higher doses at the same economic cost; however, positioning them on the right place is essential and interpretation of the efficacy should be tested first by quantitative *in vitro* screening approaches, ideally in various patient-derived cell lines. The suboptimal restored dystrophin protein levels in clinical trials were likely based on the limited uptake of PMO-SSOs into the skeletal muscle at the used low doses of, maximum, 50 mg/kg/week.[9] Indeed, we had deciphered the reason for this limited PMO uptake in earlier studies, we had shown that the uptake of the PMOs was limited to the inflammatory foci and active muscle-regenerating regions of the tissue.[25] In the inflammatory foci, PMOs enter into macrophages, activated myoblasts, and fusing myotubes.[25] Of note is also the fact that higher levels of dystrophin could be induced by increasing the PMO doses both in mice[22,23] and in humans.[35]

It has been shown that dose escalation improved the cardiac and skeletal muscle functions in *mdx* mice. Single systemic delivery of high morpholino doses (3 g/kg) induced up to 50% and 30% normal levels of dystrophin in skeletal and cardiac muscles, respectively.[22,23] Moreover, it was also shown that increasing the PMO dose induces an increase in both the number of dystrophin-positive fibers and the intensity of dystrophin signal in *mdx* mice.[22] Considering this together with the fact that younger DMD patients have relatively more inflammatory regions and active regenerating muscle fibers than late-term DMD patients suggests that younger DMD patients may benefit significantly better from higher PMO doses. Additionally, for the multi-exon-skipping concept, effective PMO dosing is critical to make it economically feasible. By using an SSO cocktail, multi-exon skipping is applicable to approximately 80% of DMD patients and offers an opportunity for drug development.[36] On the other hand, since the cumulative dose of the selected SSOs increases the cost of the treatment, determining optimal dosing and optimal SSOs with the shortest length is essential for cost reduction. Exon skipping can be also induced by editing the *cis*-acting splicing regulatory elements on the genome instead of pre-mRNA targeting. In a recent study, Amoasii et al. used adeno-associated viruses (AAVs) encoding CRISPR-Cas9 genome-editing components successfully in order to elicit exon skipping and dystrophin restoration.[37] Although genome editing is promising, it is still under preclinical development and faces similar safety concerns and challenges in clinical development as gene therapy does. It should be considered that high doses of AAV

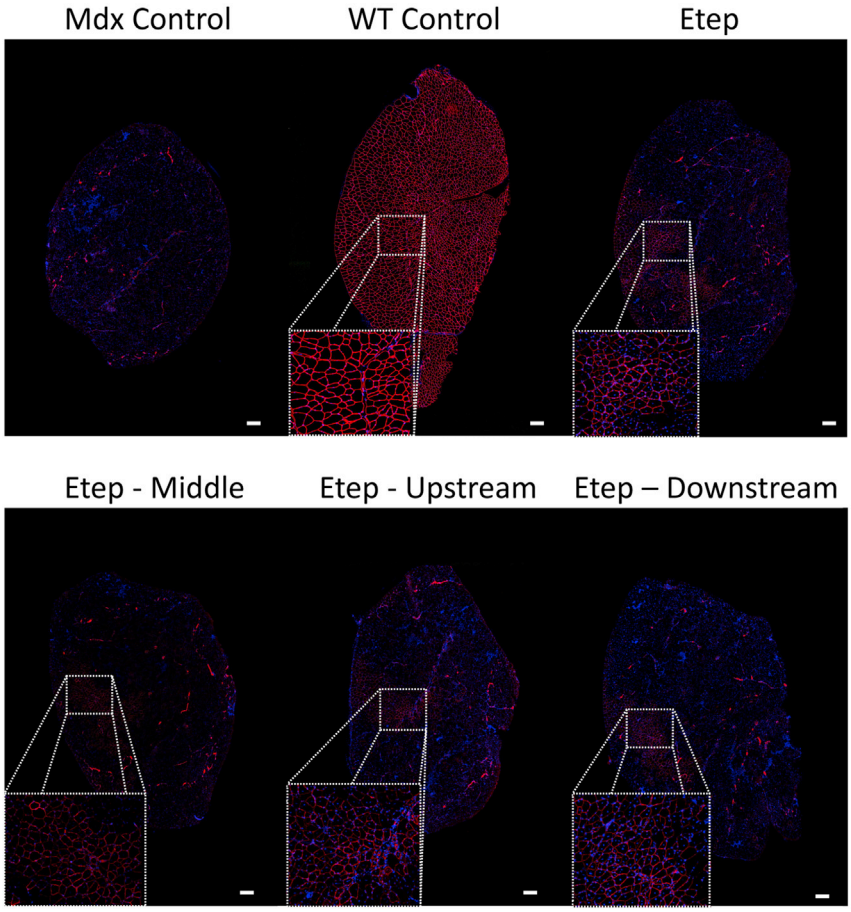

Figure 4. Validation of Restoration of Dystrophin Production by Shorter PMOs in Dystrophin-Null *mdx*52 Mice

Dystrophin expression in tibialis anterior muscles of *mdx*52 mice after intramuscular injection of 20 μg of the PMOs. Dystrophin immunoreactivity (Dys, red) was localized to the sarcolemma of myofibers, indicating exon 51 skipping and dystrophin restoration *in vivo*. Nuclei were stained with DAPI. Scale bars, 200 μm.

administration had serious toxicity issues in non-human primates and piglets.[38] Thus, the clinically tested and safe exon-skipping approach by PMOs is currently still the most feasible dystrophin-restoring treatment strategy so far for DMD patients.

MATERIALS AND METHODS

Cell Culture and PMO Transfection

In order to assess exon-skipping efficacies of the PMOs, we used conditionally immortalized mouse H2K myoblast cell lines: H2K-*mdx*52 clone 2E2C2 with the deletion mutation of exon 52 in *Dmd* and H2K-*mdx*23 clone 1A5 with a nonsense point mutation in exon 23 of *Dmd*. Both mutations create a premature stop codon in the mRNA of *Dmd*. For proliferation, myoblasts were maintained in growth medium (GM; DMEM, high glucose [GIBCO, Thermo Fisher Scientific, Gaithersburg, MD, USA], 20% fetal calf serum [Biochrom, Berlin, Germany], 0.5% chick embryo extracts [CEEs; US Biological, Salem, MA, USA], and 20 U/mL interferon (IFN)-γ [Roche, Grenzach-Wyhlen, Germany]) on Matrigel-coated dishes and kept in a humidified incubator at 33°C and 10% CO_2. For differentiation, when cells reached 80%–90% confluence, the GM was replaced by differentiation medium (DM; DMEM, 4.5 g/L glucose and 5% horse serum [Biochrom, Berlin, Germany]), and cells were placed in a humidified incubator at 37°C and 5% CO_2. Matrigel-coated dishes were prepared by incubating dishes with Matrigel at 100 μg/mL in DMEM for 1 hr at 37°C.

All PMOs were purchased from GeneTools (Philomath, OR, USA). PMOE23 (5′-GGCCAAACCTCGGCTTACCTGAAAT-3′) targets the boundary sequences of exon and intron 23 of the *Dmd* pre-mRNA. Etep (the PMO sequence of eteplirsen adjusted to the mouse genome) (5′-CTCCAACAGCAAAGAAGATGGCATTTCTAG-3′) and shorter PMOs, which are referred to as Etep-Upstream (5′-CTCCAACAGCAAAGAAGATGGCATT-3′), Etep-Middle (5′-CAACAGCAAAGAAGATGGCATTTCT-3′), and Etep-Downstream (5′-ACAGCAAAGAAGATGGCATTTCTAG-3′), target an internal sequence of exon 51 of the mouse dystrophin pre-mRNA (Figure 1). The scramble PMO (5′-CGGAACCCAGTCTGCCTAGCTAAAT-3′) was used as a control to assess the secondary effects of the morpholino chemistry and the procedures. Transfection of H2K myoblasts with the PMOs was carried out after 24 hr of induction of differentiation with varying levels of concentration of each PMO (100 nM to 3 μM and 1 μM to 10 μM) by using 6 μM Endo-Porter-Aqueous (GeneTools, Philomath, OR, USA). Thirteen hours after transfection, the medium was replaced by fresh DM to avoid cell toxicity. After 48 hr post-transfection to allow sufficient time for transcription and splicing of dystrophin pre-mRNA, cells were collected for total RNA isolation. All transfections were performed as biological triplicates to check for variability.

RNA Isolation and cDNA Synthesis

RNA was collected 48 hr after transfection to provide cells sufficient time for *Dmd* pre-mRNA splicing in the presence of the PMO, since transcription and splicing of the dystrophin mRNA takes approximately 16 hr.[39] Total RNA was isolated by using the RNeasy Mini Kit (QIAGEN, Hilden, Germany) according to the manufacturer's protocol. The RNA integrity was assessed by denaturing gel electrophoresis, and the RNA concentration was measured with the NanoDrop 3000 prior to cDNA synthesis. cDNA was synthesized

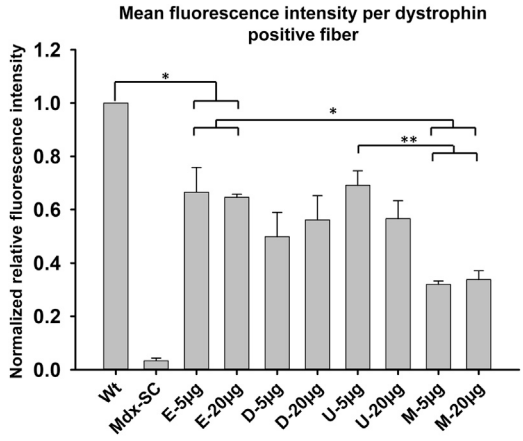

Figure 5. Comparison of the Mean Fluorescence of the Dystrophin-Positive Fibers of the PMOs and Saline-Treated *mdx52* Mice and Wild-Type Mice

Each bar represents the mean fluorescence intensity per fiber. Two mice per group were injected by an indicated dose of the PMOs. Approximately 100 dystrophin-positive fibers were analyzed per mouse. Mean intensities were calculated from the mean intensities of each specimen. Detailed analyses are represented in Figure S4 and Table S3. Wt, wild-type; SC, saline control; E, Etep; D, Etep-downstream; U, Etep-upstream; and M, Etep-middle. *$p < 0.05$; **$p < 0.01$. Error bars represent SD.

from 500 ng total RNA in a 20-μL reaction mixture, with oligo(dT) primers and SuperScript III Reverse Transcriptase (Invitrogen, Waltham, MA, USA) according to the manufacturer's protocol.

Exon-Skipping Analysis by Nested RT-PCR

Exon skipping of the H2K myoblasts after PMO transfection was assessed by the nested RT-PCR method. Nested PCR was preferred to display *Dmd* expression due to the low abundance of skipped dystrophin transcripts. The cells transfected with lower doses of the PMOs do not show the skipped band on agarose gel with 30 cycles of primary PCR reaction. Primer sequences are indicated in Table S1. Alpha-actinin expression was also assessed as the indicator of proper myogenic differentiation. Alpha-actinin expression was examined from the same cDNA pool as *Dmd* expression, instead of cDNA that was generated by the gene-specific primers, for normalization of the *Dmd* transcripts to be able to compare skipping efficacies of each PMO between different doses at equal myogenicity. The primary reaction of nested PCR and PCR of alpha-actinin was performed in a 25-μL reaction mixture with 1 μL cDNA, 1.5 mM $MgCl_2$, 200 μM dinucleotide triphosphate (dNTP) mix, 0.2 μM each of primer pair, 1× reaction buffer, and 2 U Platinum Taq DNA Polymerase (Invitrogen, Waltham, MA, USA). The following protocol was used for the reactions: 94°C for 2 min, 30 cycles of 94°C for 30 s, 55°C for 30 s, and 72°C for 1 min. The secondary reaction of nested PCR was performed in a 25-μL reaction mixture with 1 μL of the first step PCR reaction product, 2 mM $MgCl_2$, 200 μM dNTP mix, 0.2 μM each of inner primer pair, 1× reaction buffer, 1× Q-solution, and 2.5 U HotStar Taq DNA Polymerase (QIAGEN, Hilden, Germany). The following protocol was used for the inner PCR: 95°C for 15 min, 35 cycles of 91°C for 1 min, 55°C for 1 min, and 72°C for 1 min, followed by 72°C for 10 min. In all PCR runs, a no-DNA-template control (NTC) was included as a negative control. PCR products were analyzed by 2% agarose gel stained with DNA-intercalating PeqGreen dye (PEQLAB, Erlangen, Germany), and band intensity analysis was performed using ImageJ software (NIH). In order to validate the skipping of the exons, excised bands from gels were sequenced by Microsynth Seqlab Service (Göttingen, Germany).

In Vivo Validation of Exon Skipping of Shorter PMOs

All animal procedures were thoroughly reviewed and given explicit prior approval by the Institutional Animal Care and Use Committee of the Children's National Health System (CNHS) in Washington, DC. Mouse strains were initially obtained from the Jackson Laboratory (Bar Harbor, ME, USA). Mice were housed and bred at the CNHS Research Animal Facility; were provided food, water, and enrichment *ad libitum*; and were maintained under 12-hr/12-hr light/dark cycles. The *mdx52* mouse model of DMD was utilized for validation of exon skipping efficacies of shorter PMOs that target exon 51 of *Dmd* pre-mRNA. This strain lacks dystrophin expression due to the deletion mutation of exon 52 in *Dmd*. The C57BL/6 (Bl6, wild-type) mouse was used as the control where indicated. The PMOs were diluted in saline and warmed at 50°C for 15 min prior to injection. TA muscles of 6-week-old *mdx*52 mice were injected intramuscularly with 5 μg and 20 μg of each PMO. Saline was injected at an equivalent volume as a control. After 2 weeks, TA muscles were surgically removed, mounted on cork with tragacanth gum, flash-frozen in liquid-nitrogen-chilled isopentane, and stored at −80°C. Tissues were sectioned at 8 μm on a Leica CM1900 cryostat, and sections were used for immunofluorescence staining. Cryosections were stained with the anti-dystrophin antibody (GTX15277, 1:100, GeneTex, Irvine, CA, USA) and anti-laminin-α2 (4H8-2, 1:100, Enzo Life Sciences, Farmingdale, NY, USA) antibody. Staining, microscopy, and image acquisition were performed as previously described.[25]

Statistical Analyses

Relative intensities of the PCR products in agarose gels were quantified by ImageJ software (NIH). The intensities of *Dmd* transcripts under PMO treatment were normalized to the corresponding intensity of alpha-actinin transcript, and then further normalized to the intensity of *Dmd* transcript from the scramble PMO. Dixon's Q test was applied for identification and rejection of outliers from biological replicates. The resulting value was referred to as the "normalized relative expression." Skipping percentage was calculated as (normalized relative expression of the skipped transcript/[normalized relative expression of the skipped + normalized relative expression of the unskipped transcripts]) × 100.

Normalized relative expressions of skipped and unskipped transcripts were plotted against the concentration series of each PMO. While dose-response curves of unskipped transcripts were fitted to a hyperbolic decay curve with 3 parameters (R2 = 0.93–0.99), dose-response curves of skipped transcripts were fitted to a single rectangular II curve with 3 parameters (R2 = 0.84–0.97) by Sigmaplot v12.5

software. Curve equations and coefficient values were generated by Sigmaplot v12.5 software. Expression levels of both skipped and unskipped transcripts that were at the same quantity in response to each PMO were determined by finding the intersection point of the curves from the curve equations.

Quantification of dystrophin-positive fibers and semi-quantification of fluorescence intensity of dystrophin expression were performed on TA muscles of *mdx* mice treated, as described earlier[8,40], by ImageJ software (NIH). Percentages of dystrophin-positive fibers of stained sections were calculated based on the following formula: (total dystrophin positive fibers/total laminin-positive fibers) × 100. Semiquantitative measurements of dystrophin expression were carried out for approximately 100 fibers from three to four different regions of each muscle section. The analysis of the mean fluorescence intensity per dystrophin-positive fiber was performed similarly to established methodologies.[8,40] Briefly, dystrophin intensity of each fiber was normalized to laminin intensity of the fiber, and then the dystrophin/laminin intensity value of the PMO-treated fibers was normalized to the mean of dystrophin/laminin intensity value of wild-type mouse. All muscle images that were used for quantification of dystrophin-positive fibers and semi-quantification of fluorescence intensity of dystrophin expression are provided in the Supplemental Information.

SUPPLEMENTAL INFORMATION

Supplemental Information includes four figures, three tables, and muscle images and can be found with this article online at https://doi.org/10.1016/j.omtn.2018.10.002.

AUTHOR CONTRIBUTIONS

U.A. conducted the *in vitro* experiment, analyzed data and wrote the manuscript. H.W. and K.B. collected *in vitro and in vivo* data. T.A.P. and A.C. critically reviewed the manuscript. J.S.N. conducted the intramuscular injections. S.C. designed the study, obtained funding, supervised the experiments, and wrote the manuscript. All authors reviewed the manuscript.

CONFLICTS OF INTEREST

The authors have no conflicts of interest.

ACKNOWLEDGMENTS

This work was funded by the Deutsche Forschungsgemeinschaft through an Emmy Noether grant (CI 218/1-1) to S.C., the Muscular Dystrophy Association (MDA295203) to T.A.P. and S.C., and an NIH NIAMS Genetics and Genomics of Muscle Postdoctoral Training grant (T32AR056993) to J.S.N. The International Postdoctoral Research Fellowship Programme of the TUBITAK supported U.A. (1059B191501880).

REFERENCES

1. Hoffman, E.P., Brown, R.H., Jr., and Kunkel, L.M. (1987). Dystrophin: the protein product of the Duchenne muscular dystrophy locus. Cell *51*, 919–928.

2. Koenig, M., Hoffman, E.P., Bertelson, C.J., Monaco, A.P., Feener, C., and Kunkel, L.M. (1987). Complete cloning of the Duchenne muscular dystrophy (DMD) cDNA and preliminary genomic organization of the DMD gene in normal and affected individuals. Cell *50*, 509–517.

3. Flanigan, K.M., Dunn, D.M., von Niederhausern, A., Soltanzadeh, P., Gappmaier, E., Howard, M.T., Sampson, J.B., Mendell, J.R., Wall, C., King, W.M., et al.; United Dystrophinopathy Project Consortium (2009). Mutational spectrum of DMD mutations in dystrophinopathy patients: application of modern diagnostic techniques to a large cohort. Hum. Mutat. *30*, 1657–1666.

4. Ervasti, J.M., and Campbell, K.P. (1993). A role for the dystrophin-glycoprotein complex as a transmembrane linker between laminin and actin. J. Cell Biol. *122*, 809–823.

5. Ibraghimov-Beskrovnaya, O., Ervasti, J.M., Leveille, C.J., Slaughter, C.A., Sernett, S.W., and Campbell, K.P. (1992). Primary structure of dystrophin-associated glycoproteins linking dystrophin to the extracellular matrix. Nature *355*, 696–702.

6. Cirak, S., Feng, L., Anthony, K., Arechavala-Gomeza, V., Torelli, S., Sewry, C., Morgan, J.E., and Muntoni, F. (2012). Restoration of the dystrophin-associated glycoprotein complex after exon skipping therapy in Duchenne muscular dystrophy. Mol. Ther. *20*, 462–467.

7. Anthony, K., Cirak, S., Torelli, S., Tasca, G., Feng, L., Arechavala-Gomeza, V., Armaroli, A., Guglieri, M., Straathof, C.S., Verschuuren, J.J., et al. (2011). Dystrophin quantification and clinical correlations in Becker muscular dystrophy: implications for clinical trials. Brain *134*, 3547–3559.

8. Cirak, S., Arechavala-Gomeza, V., Guglieri, M., Feng, L., Torelli, S., Anthony, K., Abbs, S., Garralda, M.E., Bourke, J., Wells, D.J., et al. (2011). Exon skipping and dystrophin restoration in patients with Duchenne muscular dystrophy after systemic phosphorodiamidate morpholino oligomer treatment: an open-label, phase 2, dose-escalation study. Lancet *378*, 595–605.

9. Mendell, J.R., Rodino-Klapac, L.R., Sahenk, Z., Roush, K., Bird, L., Lowes, L.P., Alfano, L., Gomez, A.M., Lewis, S., Kota, J., et al.; Eteplirsen Study Group (2013). Eteplirsen for the treatment of Duchenne muscular dystrophy. Ann. Neurol. *74*, 637–647.

10. Bello, L., Morgenroth, L.P., Gordish-Dressman, H., Hoffman, E.P., McDonald, C.M., and Cirak, S.; CINRG Investigators (2016). DMD genotypes and loss of ambulation in the CINRG Duchenne Natural History Study. Neurology *87*, 401–409.

11. Bello, L., and Pegoraro, E. (2016). Genetic diagnosis as a tool for personalized treatment of Duchenne muscular dystrophy. Acta Myol. *35*, 122–127.

12. Mann, C.J., Honeyman, K., Cheng, A.J., Ly, T., Lloyd, F., Fletcher, S., Morgan, J.E., Partridge, T.A., and Wilton, S.D. (2001). Antisense-induced exon skipping and synthesis of dystrophin in the *mdx* mouse. Proc. Natl. Acad. Sci. USA *98*, 42–47.

13. van Deutekom, J.C., Bremmer-Bout, M., Janson, A.A., Ginjaar, I.B., Baas, F., den Dunnen, J.T., and van Ommen, G.J. (2001). Antisense-induced exon skipping restores dystrophin expression in DMD patient derived muscle cells. Hum. Mol. Genet. *10*, 1547–1554.

14. Arechavala-Gomeza, V., Graham, I.R., Popplewell, L.J., Adams, A.M., Aartsma-Rus, A., Kinali, M., Morgan, J.E., van Deutekom, J.C., Wilton, S.D., Dickson, G., and Muntoni, F. (2007). Comparative analysis of antisense oligonucleotide sequences for targeted skipping of exon 51 during dystrophin pre-mRNA splicing in human muscle. Hum. Gene Ther. *18*, 798–810.

15. Harding, P.L., Fall, A.M., Honeyman, K., Fletcher, S., and Wilton, S.D. (2007). The influence of antisense oligonucleotide length on dystrophin exon skipping. Mol. Ther. *15*, 157–166.

16. Goemans, N.M., Tulinius, M., van den Akker, J.T., Burm, B.E., Ekhart, P.F., Heuvelmans, N., Holling, T., Janson, A.A., Platenburg, G.J., Sipkens, J.A., et al. (2011). Systemic administration of PRO051 in Duchenne's muscular dystrophy. N. Engl. J. Med. *364*, 1513–1522.

17. Hoffman, E.P., Bronson, A., Levin, A.A., Takeda, S., Yokota, T., Baudy, A.R., and Connor, E.M. (2011). Restoring dystrophin expression in duchenne muscular dystrophy muscle progress in exon skipping and stop codon read through. Am. J. Pathol. *179*, 12–22.

18. Goemans, N.M., Tulinius, M., van den Hauwe, M., Kroksmark, A.K., Buyse, G., Wilson, R.J., van Deutekom, J.C., de Kimpe, S.J., Lourbakos, A., and Campion, G. (2016). Long-term efficacy, safety, and pharmacokinetics of drisapersen in

Duchenne muscular dystrophy: results from an open-label extension study. PLoS ONE *11*, e0161955.

19. Lu, Q.L., Cirak, S., and Partridge, T. (2014). What can we learn from clinical trials of exon skipping for DMD? Mol. Ther. Nucleic Acids *3*, e152.
20. Lim, K.R., Maruyama, R., and Yokota, T. (2017). Eteplirsen in the treatment of Duchenne muscular dystrophy. Drug Des. Devel. Ther. *11*, 533–545.
21. Willer, T., Lee, H., Lommel, M., Yoshida-Moriguchi, T., de Bernabe, D.B., Venzke, D., Cirak, S., Schachter, H., Vajsar, J., Voit, T., et al. (2012). ISPD loss-of-function mutations disrupt dystroglycan O-mannosylation and cause Walker-Warburg syndrome. Nat. Genet. *44*, 575–580.
22. Wu, B., Lu, P., Benrashid, E., Malik, S., Ashar, J., Doran, T.J., and Lu, Q.L. (2010). Dose-dependent restoration of dystrophin expression in cardiac muscle of dystrophic mice by systemically delivered morpholino. Gene Ther. *17*, 132–140.
23. Wu, B., Xiao, B., Cloer, C., Shaban, M., Sali, A., Lu, P., Li, J., Nagaraju, K., Xiao, X., and Lu, Q.L. (2011). One-year treatment of morpholino antisense oligomer improves skeletal and cardiac muscle functions in dystrophic mdx mice. Mol. Ther. *19*, 576–583.
24. Sazani, P., Weller, D.L., and Shrewsbury, S.B. (2010). Safety pharmacology and genotoxicity evaluation of AVI-4658. Int. J. Toxicol. *29*, 143–156.
25. Novak, J.S., Hogarth, M.W., Boehler, J.F., Nearing, M., Vila, M.C., Heredia, R., Fiorillo, A.A., Zhang, A., Hathout, Y., Hoffman, E.P., et al. (2017). Myoblasts and macrophages are required for therapeutic morpholino antisense oligonucleotide delivery to dystrophic muscle. Nat. Commun. *8*, 941.
26. van den Bergen, J.C., Wokke, B.H., Janson, A.A., van Duinen, S.G., Hulsker, M.A., Ginjaar, H.B., van Deutekom, J.C., Aartsma-Rus, A., Kan, H.E., and Verschuuren, J.J. (2014). Dystrophin levels and clinical severity in Becker muscular dystrophy patients. J. Neurol. Neurosurg. Psychiatry *85*, 747–753.
27. Pandya-Jones, A. (2011). Pre-mRNA splicing during transcription in the mammalian system. Wiley Interdiscip. Rev. RNA *2*, 700–717.
28. Wee, K.B., Pramono, Z.A., Wang, J.L., MacDorman, K.F., Lai, P.S., and Yee, W.C. (2008). Dynamics of co-transcriptional pre-mRNA folding influences the induction of dystrophin exon skipping by antisense oligonucleotides. PLoS ONE *3*, e1844.
29. Aartsma-Rus, A., van Vliet, L., Hirschi, M., Janson, A.A., Heemskerk, H., de Winter, C.L., de Kimpe, S., van Deutekom, J.C., 't Hoen, P.A., and van Ommen, G.J. (2009). Guidelines for antisense oligonucleotide design and insight into splice-modulating mechanisms. Mol. Ther. *17*, 548–553.
30. Echigoya, Y., Lim, K.R.Q., Trieu, N., Bao, B., Miskew Nichols, B., Vila, M.C., Novak, J.S., Hara, Y., Lee, J., Touznik, A., et al. (2017). Quantitative antisense screening and optimization for exon 51 skipping in Duchenne muscular dystrophy. Mol. Ther. *25*, 2561–2572.
31. Echigoya, Y., Mouly, V., Garcia, L., Yokota, T., and Duddy, W. (2015). In silico screening based on predictive algorithms as a design tool for exon skipping oligonucleotides in Duchenne muscular dystrophy. PLoS ONE *10*, e0120058.
32. Pires, V.B., Simões, R., Mamchaoui, K., Carvalho, C., and Carmo-Fonseca, M. (2017). Short (16-mer) locked nucleic acid splice-switching oligonucleotides restore dystrophin production in Duchenne Muscular Dystrophy myotubes. PLoS ONE *12*, e0181065.
33. Aartsma-Rus, A., Houlleberghs, H., van Deutekom, J.C., van Ommen, G.J., and 't Hoen, P.A. (2010). Exonic sequences provide better targets for antisense oligonucleotides than splice site sequences in the modulation of Duchenne muscular dystrophy splicing. Oligonucleotides *20*, 69–77.
34. Popplewell, L.J., Trollet, C., Dickson, G., and Graham, I.R. (2009). Design of phosphorodiamidate morpholino oligomers (PMOs) for the induction of exon skipping of the human DMD gene. Mol. Ther. *17*, 554–561.
35. Komaki, H., Nagata, T., Saito, T., Masuda, S., Takeshita, E., Sasaki, M., Tachimori, H., Nakamura, H., Aoki, Y., and Takeda, S. (2018). Systemic administration of the antisense oligonucleotide NS-065/NCNP-01 for skipping of exon 53 in patients with Duchenne muscular dystrophy. Sci. Transl. Med. *10*, eaan0713.
36. Aslesh, T., Maruyama, R., and Yokota, T. (2018). Skipping multiple exons to treat DMD—promises and challenges. Biomedicines *6*, E1.
37. Amoasii, L., Long, C., Li, H., Mireault, A.A., Shelton, J.M., Sanchez-Ortiz, E., McAnally, J.R., Bhattacharyya, S., Schmidt, F., Grimm, D., et al. (2017). Single-cut genome editing restores dystrophin expression in a new mouse model of muscular dystrophy. Sci. Transl. Med. *9*, eaan8081.
38. Hinderer, C., Katz, N., Buza, E.L., Dyer, C., Goode, T., Bell, P., Richman, L.K., and Wilson, J.M. (2018). Severe toxicity in nonhuman primates and piglets following high-dose intravenous administration of an adeno-associated virus vector expressing human SMN. Hum. Gene Ther. *29*, 285–298.
39. Tennyson, C.N., Klamut, H.J., and Worton, R.G. (1995). The human dystrophin gene requires 16 hours to be transcribed and is cotranscriptionally spliced. Nat. Genet. *9*, 184–190.
40. Arechavala-Gomeza, V., Kinali, M., Feng, L., Brown, S.C., Sewry, C., Morgan, J.E., and Muntoni, F. (2010). Immunohistological intensity measurements as a tool to assess sarcolemma-associated protein expression. Neuropathol. Appl. Neurobiol. *36*, 265–274.